

Refractories Applications *Transactions*

Volume 2, Number 1

July/August 2006

Editorial Board

Jeffrey D. Smith, Editor, University of Missouri-Rolla, USA
Mary Lee, Assistant to the Editor, University of Missouri-Rolla, USA
William Headrick, University of Missouri-Rolla, USA
Musa Karakus, University of Missouri-Rolla, USA

Technical Referees

Esteban Aglietti, CETMC, Argentina
Richard C. Bradt, The University of Alabama, USA
Carmen Baudín, Instituto de Cerámica y Vidrio, Spain
Elena Brandaleze, Instituto Argentino de Siderurgia
Angel Caballero, Instituto de Cerámica y Vidrio, Madrid, Spain
William G. Fahrenholtz, University of Missouri-Rolla, USA
Geraldo E. Gonçalves, Magnesita S.A., Brazil
J.P. Guha, University of Missouri-Rolla, USA
Orville Hunter, Consultant, USA
William E. Lee, Imperial College London, UK
Li Nan, Wuhan University of Sci. & Tech., China
George Oprea, The University of British Columbia, Canada
Victor C. Pandolfelli, Universidade Federal de São Carlos, Brazil
Christopher Parr, Lafarge Aluminates, France
Jacques Poirier, Polytech, Orleans, France
Michel Rigaud, École Polytechnique, Canada
Charles Semler, Semler Materials Services, USA
Mark Stett, Consultant, USA
Raul Topolevsky, Siderar, Argentina

All submissions should be sent to:

Mary Lee, Assistant to the Editor
Refractories Applications Transactions
University of Missouri-Rolla
Materials Science and Engineering Dept.
223 McNutt Hall
1870 Miner Circle Drive
Rolla, MO 65409-0330

Phone: (573) 341-6561
Fax: (573) 341-6934
E-mail: leem@umr.edu

For author guidelines please see those listed on the *Journal of the American Ceramic Society* website: <http://www.ceramics.org/publications/journal/authorinstructions.asp>

File Formats

Text: Microsoft Word.

Graphics: JPEG, TIFF or EPS created from supported applications, PowerPoint, Acrobat PDF (PDF format is acceptable for review purposes only)

Microsoft Word with embedded graphics.

Compression Software: WinZip (PC) or Stuffit (Macintosh)

Resolution of graphics files must be at least 300 dpi for halftones, 600 dpi for lettering, and 1200 dpi for line art.

Influence of Aging Time on Rheological Behavior of Bauxite-Based Low-Cement Pumpable Castables

Xianxin Zhou, K. Sankaranarayanan and Michel Rigaud
École Polytechnique de Montreal, QC, Canada H3C 3A7

Ningsheng Zhou High Temperature Materials Institute., Henan University of Science and Technology,
48 Xiyuan Road, Luoyang, Henan 471003, P.R. China

ABSTRACT

Effect of aging time on rheological behavior of bauxite-based low-cement pumpable castable has been studied in detail with two different rheometers, one for the castable and the other for the fine matrix. With time, three stages have been distinguished; homogenization, saturation and setting. The flow resistance decreased during homogenization, remained stable during saturation and increased during setting. This trend is expressed through conductivity and exothermic profile studies on the fine matrix and whole castable, respectively.

1. INTRODUCTION

There are many studies of hydration of calcium aluminate cement (CAC) and the setting mechanism of low cement castables (LCC) explaining the hydration process of CAC in castable.^{1,2,3,4,5,6} The mechanism of hydration of calcium aluminate cement starts with dissolution of the CAC constituents by various hydrate formation, followed by precipitation of the hydrates from solution. The hydration process can be divided into three stages: (a) dissolution, (b) nucleation and (c) massive precipitation and crystallization.

Rheological characteristics can be expressed by the relationships between shear stress (τ) and shear rate ($\dot{\gamma}$), apparent viscosity (η) and shear rate and apparent viscosity versus time under a constant shear rate. Behavior of a fluid can be understood using flow curves (τ - $\dot{\gamma}$ or η - $\dot{\gamma}$ curves). As described previously,^{7,8} there are six flow patterns in a narrow range of shear rates: Newtonian, Bingham (or yield-Newtonian), Pseudoplastic, Yield-Pseudoplastic (plastic flow), Dilatant and Yield-Dilatant. Since dilatancy or shear-thickening causes problems during installation, dilatant flow is an undesirable behavior for castable. Castables commonly follow a Bingham or shear-thinning behavior⁹, with a yield stress τ_y . For an applied stress $\tau \leq \tau_y$, no flow occurs; when $\tau \geq \tau_y$, plastic flow occurs. For self-flow castables, τ_y is overcome by gravitational force on the castable making the castable self-level without application of another external force. Rheology may be expressed by the Herschel-Bulkley equation that incorporates the elements of Newtonian, Bingham and power laws (Ostwald model),^{10,11,12,13} as follows:

$$\tau = \tau_y + (\eta_p \cdot \dot{\gamma}^n) \quad (1)$$

where, τ is shear stress (Pa), τ_y is plastic yield stress (Pa), η_p is plastic (Bingham) viscosity (Pa·s), $\dot{\gamma}$ is shear rate, (s^{-1}) and n is the power law index of the material.

When $n = 1$ and $\tau_y = 0$, the equation describes a Newtonian fluid; when $n = 1$ and $\tau_y > 0$, a Bingham and when $n < 1$ and $\tau_y > 0$, a yield-pseudoplastic. Mathematically, Bingham rheology differs from yield-pseudoplastic, but in practice they are quite similar. A yield-pseudoplastic rheology may really be Bingham, but the rheogram may not have been measured at sufficiently high shear rates to detect the constant, high shear, plastic viscosity. Such a flow

pattern corresponds to a shear-thinning effect, which is desirable for casting by vibration. During vibration, castables should easily flow to fill a cavity, during which the entrapped air should escape avoiding large pores. This flowability should result from thixotropy, rather than from excess water, since in the latter case the porosity of the placed body is too high and segregation may occur. After casting, when vibration stops, the cast structure should soon settle to prevent segregation of the coarse aggregates.⁹

When CAC reacts with water to form a hydrate, heat is evolved. Most hydration reactions end in a short time, concentrating the heat of hydration to this period. The cement hydration process has been defined and quantified by different techniques, such as mixing energy, conductimetry and calorimetry.^{3,14,15,16} This hydration process in cement bonded castables must consider all interactions or interferences, mixing CAC, micro-silica, other fine fillers, dispersants and water. It is evident that no single technique is able to provide a complete understanding of the interactions that occur within castables during their placement. More predictive techniques are required for an efficient optimization of castable installation characteristics.³

In practice, two important characteristics of castables are considered: working time and setting time. Working time of a castable is the time after mixing until which the castable can still be well placed by vibration or self-flowing. An industrial installation needs at least 45 min of working time. There are ASTM standards to evaluate working time of both vibration and self-flow castables. Usually a flow decay test is used to assess the working time of self-flow castable.^{17,18,19,20} Flow decay is the time required to reach zero free-flow after wet mixing. For a castable, set time is influenced not only by the individual characteristics of the raw materials, but to a large extent by synergistic interactions between individual components. This makes it almost impossible to predict the behavior without testing. It is relatively easy to measure flowability by the flow table test using a cone described in ASTM C1445-99.²¹ In ASTM C 1446-99, working time of self-flowing castable is defined as the elapsed time from the first addition of water or liquid during mixing until the mix will only achieve 25% self-flow using the procedure described in this test method. Self-flowability of 25% has been selected as the minimum at which a mix can be poured into typical molds or forms in normal practice. Typically flow decay is tested until zero self-flow is achieved, instead of 25% flow. This test method is not appropriate or sufficient for determining the pumpability of castable refractories. As the attempts to predict the pumpability from self-flowability test alone are not always successful, the rheological properties of a castable against time must be considered.

In castable research, it is common to evaluate the rheological behavior of the matrix and to correlate the data with the behavior of castable. It is an inadequate approach and further efforts are required to evaluate rheology of castable as well. After the introduction of coarse grains into fine matrix, the rheology may change due to effects such as absorption of a portion of water by grains, or grain anisotropy or shape factors. It is then more appropriate to evaluate the rheology of both fine matrix slurry and castable and correlate them. Pandolfelli showed that refractory castable rheology is significantly influenced by mixing method, particle size distribution and water-addition.²²⁻²³ In this work, the rheology of the castable is investigated in terms of the rheo-

logical parameters flow resistance (G) and torque viscosity (H)^{24,26} and matrix rheology with plastic yield stress (τ_y) and plastic viscosity (η_p) against time. The correlations between these parameters are then analyzed and also complemented by ionic conductivity and exothermal profile determinations.

2. EXPERIMENTAL

2.1 Materials

Chinese high-grade bauxite (3.40g/cm³ bulk density and 85.1% Al₂O₃ content) was used as coarse aggregate, with size fractions of 5-3 mm, 3-1 mm and 1-0.21 mm, as supplied from Henan Gengsheng Refractories Co. Ltd., China. Three kinds of bauxite fines with the same quality but different particle size distribution (PSD), microsilica 971U (Elkem Materials, Norway), calcium aluminate cement CA-14 (Almatis, USA) were all used as fine fillers. The median (d_{50}) particle size was 25.55 μ m, 12.80 μ m and 5.45 μ m for Bauxite-1, Bauxite-2 and Bauxite-3, respectively. All the bauxite fines were monomodal in size distribution and the submicron ($d < 1 \mu$ m) content is around 7.0 vol%. Sodium hexametaphosphate (SHMP) was used as dispersant.

The castable composition is given in **Table 1**. The PSD of the castable mixes were designed according to Andreasen's equation⁷ as given below:

$$CPFT = 100 (d / D_{max})^q \quad (2)$$

where CPFT is particle cumulative percent finer than (vol%), D is particle size (mm), D_L is largest particle size (mm) and q is distribution modulus.

The castable with a q value of 0.26 and a D_{max} of 5 mm was chosen for this study.²⁴ The cement and microsilica contents were fixed at 4 and 5 wt%, respectively, since such a formulation provided satisfactory results in previous investigations.²⁵ The amount of water was fixed at 7 wt% and sodium hexametaphosphate (SHMP) was added at 0.12 wt% which corresponds to a self-flowability of 120%. This castable showed good workability and pumpability in shotcreting trials.²

2.2 IBB Rheometer for Castable Rheology

A rheometer (IBB Rheometer V1.0) was used to measure the rheology of the castable. It consists of a sampling bowl (the inner diameter 168 mm and height 200 mm) and a 3/4 HP motor, which drives an H-shape impeller (height 85 mm and width 53 mm) with a planetary motion inside the bowl. Originally developed for the rheological measurements of concretes,^{11,12,27} this rheometer has been proven to be a useful tool for refractory castables.^{24,26} Measurements are made directly on castable, whereas a viscometer can only measure the rheology of the fine matrix portion. The rheometer parameters are related through the following equation:

$$T = G + (H \cdot N) \quad (3)$$

where T is torque required to drive the impeller (Nm), G is flow resistance (Nm), N is impeller angular speed (s⁻¹) and H is torque viscosity (Nm•s).

By proper calibration, the G and H parameters can be used to calculate the fundamental rheological properties yield stress (τ_0) and apparent viscosity (η). These relate directly to the castable mobility and flow-related properties. All castable rheological tests were carried out at 20°C (environmental temperature) and the mixes were not protected from evaporation.

2.3 Bohlin Rheometer for Matrix Rheology

A CVO 120 High Resolution rheometer (Bohlin Instruments UK) was used to measure the rheology of the matrix portion of the castable defined in **Table 1**. It has an automated gap setting and control system and an interchangeable temperature control system. This viscometer is a powerful tool for suspension rheology characterization with very broad shear rate range from 0.05225 to 3344 s⁻¹ and wide temperature range up to 550°C.

The system consists of a rotating bob (inner cylinder) located in a fixed cup (outer cylinder) with the sample contained in the annular gap between them. A 25 mm diameter and 37.5 mm height bob and a coaxial 27.5 mm diameter

Table 1. Mix details for aging time study.

Aggregate (wt%)	Bauxite	59
Fine Matrix (wt%)	Bauxite-1	11
	Bauxite-2	12
	Bauxite-3	9
	CA-14 Cement	4
	Elkem-971U Microsilica	5
	SHMP Dispersant	0.12
Water addition (wt%)		7.0
Rheology testing time (castable)	Total time (min)	185
	Interval time (min)	5
Rheology testing time (matrix slurry)	Total time (h)	6
	Interval time (h)	1

and 49.9 mm working-height cup were used. A motor drives the inner cylinder. A viscosity related torque, caused by the resistance of the sample to shearing, acts on the inner cylinder. Varying the rotation speed allows apparent viscosity to be calculated using the following formula:

$$\eta = \tau / \dot{\gamma} \quad (4)$$

where τ is shear stress (Pa), $\dot{\gamma}$ is shear rate (s⁻¹) and η is apparent viscosity (Pa•s). The shear rate/shear stress and apparent viscosity/shear rate flow curves can then be generated. Viscosity and flow can be expressed as a function of time, temperature and shear rate.

2.4 Sample Preparation and Testing

Each castable was dry mixed for 5 min in a Hobart mixer and then water was added. At first, 80% of the total water was added and mixed for 3 min. The remaining water was then added and further mixed for 3 min.

Self-flowability measurements were performed as per ASTM C1446-99.²¹ For flow decay tests, 4 kg of castable was prepared and stored in an airtight container. The self-flowability was measured at 10 min intervals (a sample of around 0.5 kg was drawn from the container and returned to the container after measurement). Between measurements, the container was sealed to prevent moisture evaporation. This procedure was repeated until the castable ceased to self-flow.

For castable rheological measurements, 8 kg of castable was poured into the IBB rheometer bowl and the torque-speed relationship was observed at intervals of 5 min for a total duration of 185 min. During testing, the rotation speed of impeller was changed step-wise, and in each step the required torque and the impeller speed were measured and recorded.

For matrix rheological measurements, 205 grams of fine matrix (corresponding to fine matrix of 0.5 kg of castable) was wet-mixed in a CAFRAMO mixer at a constant speed of 200/rpm for 5 min. The water addition and dispersant dosage were kept the same as in the castable. The fresh matrix slurry was stored in a small sealed container during testing. The Bohlin Viscometer was set in isothermal mode at 20°C for all tests. Matrix slurry (12 ml) was injected into the cup of this viscometer by a syringe and then mineral oil with very low density and low viscosity was added on the top of the sample in the cup as a barrier to prevent moisture evaporation. This oil was immiscible and remained on top of the sample during testing. Measurements were performed with preset step-wise shear rates to achieve up/down sweeps at intervals of 1 h for each test. Six tests lasting a total of six hours each were performed on the slurry. The slurry for each test was taken from the container into the viscometer after cleaning the cup. The shear stress vs. time test of the matrix slurry was also performed at different shear rate levels of 0.3139, 3.094, 12.93, 30.49, 127.4 and 300.5/s, for 15 min respectively.

For conductivity measurement, matrix slurry was prepared with 41.0 g dry matrix mixed in 102.5 g water (water/solid content = 2.5). Conductivity was

measured using a pH and Conductivity Meter (Hanna Instruments) at 20°C. The measurements were made for 12 h at 5 min intervals.

For exothermic profile measurements, 3.5 kg of castable was placed into an airtight container, inside an insulated box. Two thermocouples were used to simultaneously measure the temperature at 10 seconds intervals. One was inserted into the mix and the other was used to measure room temperature.

3. RESULTS AND DISCUSSION

3.1 Castable

Self-flowability decreased as a function of time as shown in **Fig. 1**. At 25% self-flowability, the working time, according to ASTM C 1446-99, is 220 min. At 100 min, the self-flowability decreased to 100% and then reduced to 0% at around 275 min. The first 100 min was the working time and the following 175 min was the interval where gelling occurred progressively.^{14,19}

Rheometer data for the castable are shown in **Fig. 2**. At 0 min (tested immediately after pouring in bowl), the forward cycle revealed pseudoplastic behavior; while in the reverse cycle the castable approached a Bingham behavior (Newtonian-type with yield). In the forward cycle, as the impeller revolution was increased, the torque increased as the mix became more homogenized. Once the maximum testing speed was reached, the homogeneous mix behaved almost linearly in the reverse cycle. In the same test, after 5 min of mixing, there was a drastic reduction in the area of the hysteresis loop between the forward and reverse cycle. The loop area remained almost the same from 10 to 50 min, as the curves shifted downward. After 50 min, the upward/downward curves remained the same up to 150 min. After 155 min, the rheograms shifted upward and the loop area increased until the end of the test. These different rates of torque change with speed leading to different G

and H values will be discussed later. The important point to be noted is that these changes could not be observed in the flow decay test, which indicated only a gradual flow decay.

The interpretation of those observations is that at the beginning of the test, the mix was not completely homogeneous. The shearing stress broke up agglomerates, which filled voids and improved dispersion. Once the test reached the maximum speed, the mix was in a more homogeneous state and showed Bingham behavior in the reverse cycle. Further on, in the testing cycle, the mix was more homogeneous and reached a state after 50 min where further homogenization is not possible. After 150 min, the rheograms started shifting upward due to setting. These observations are consistent with the conductivity and exothermic profile studies to be detailed later.

The detailed rheometer results within the period of 185 min with a 5-minute testing interval were recorded. Data for the first 50 minutes are shown in **Fig. 3**. The hysteresis loops in this data represent the relationship between torque and impeller speed for the castable mix. The loops shift downward during 0 to 50 min as shown in **Fig. 3**, and then overlap in the time range between 50 and 100 min. The loops remain unchanged and merge in the period of 100 to 150 min and slightly rewind in the time interval of 150 to 185 min. The torque (T_{max}) at the highest impeller speed of 1.10 s^{-1} , at different testing time, is given in **Table 2**. The T_{max} decreased 33% in the first period of 50 min, slightly decreased from 50 to 100 min, remained the same from 100 to 150 min and increased from 150 to 185 min. The loop profiles change in much the same trend as T_{max} values.

The relationship between equivalent apparent viscosity and impeller speed from 0 to 50 min of testing is shown in **Fig. 4**. Typical Bingham behavior is observed. The values of equivalent apparent viscosity are calculated from the instantaneous torque divided by impeller speed. Although they are not fundamental parameters of apparent viscosity, they represent values of apparent viscosity if the data are converted appropriately. The trends are the same with other testing times and hence the data are not shown.

Though the mixes acted as Bingham fluids, when analyzed as a function of time at constant impeller speed, the mixes displayed thixotropy. Thixotropy is defined as the decrease of viscosity with time at a constant shear rate.⁷ **Fig. 5** shows the equivalent apparent viscosity calculated for the higher (1.10 s^{-1}) and lower speed (0.48 s^{-1}) respectively (in the reverse cycle of the hysteresis loops) at each five-minute cycle. It is observed that the equivalent apparent viscosity at 1.10 s^{-1} was always lower than the value at 0.48 s^{-1} . At high speed, there was a reduction of about 9.4% after initial mixing and approxi-

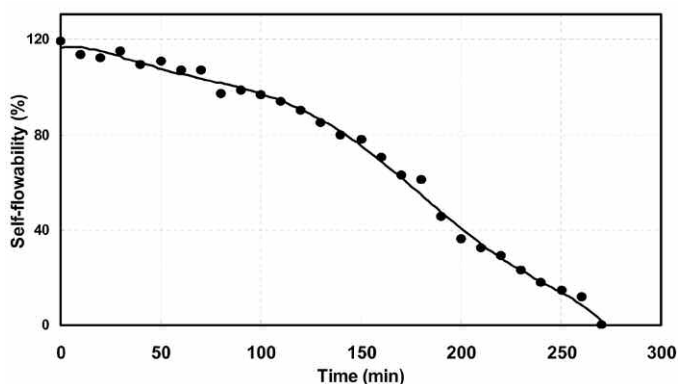


Fig. 1. Flow decay data for the castable mix.

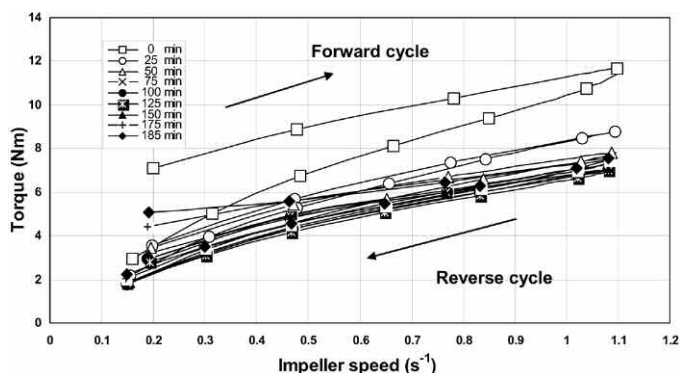


Fig. 2. Torque vs. impeller speed for 0-185 min.

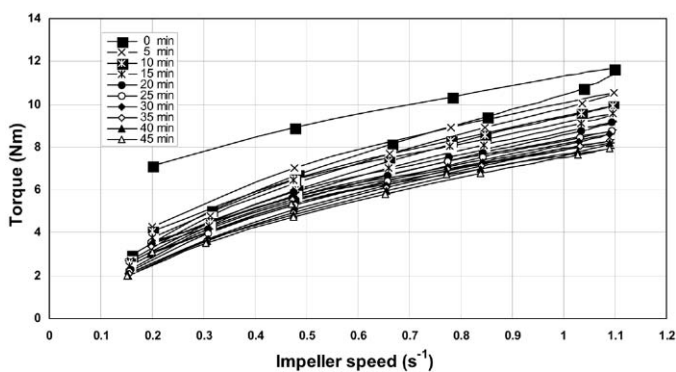


Fig. 3. Torque vs. impeller speed for 0-45 min.

Table 2. T_{max} at highest impeller speed of (1.10 s^{-1}) for selected times

Time (min)	0	25	50	75	100	125	150	175	185
T_{max} (Nm)	10.65	8.78	7.79	7.28	7.05	7.01	7.06	7.44	7.57

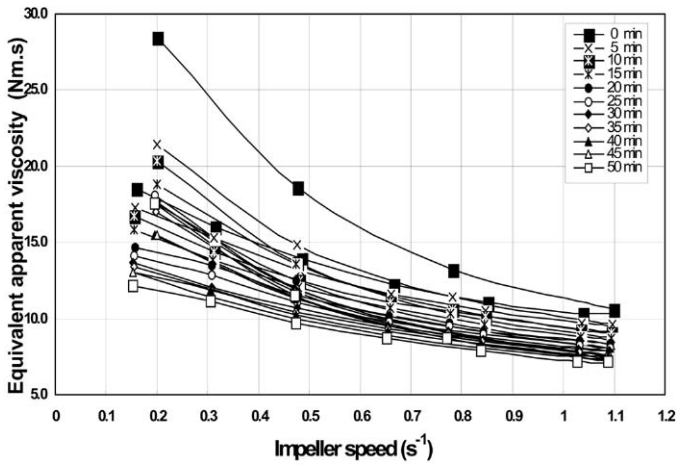


Fig. 4. Equivalent apparent viscosity vs. impeller speed for 0-50 min.

mately 26% and 35% for 30 min and 150 min, respectively. After 150 min, an 8% difference remained. The same trend was observed at low speed. The change of equivalent apparent viscosity with testing time is correlated with the hydration behavior in a later section.

The method of evaluating G and H values, using the rheometer test results, has been described elsewhere.^{24,26} The calculated values of G and H are plotted in Fig. 6. The values of G decreased by 38% at 50 min of testing and remained almost constant from 50 to 150 min. There was an increase of about 29% after 150 min until the end of the test. These ranges correspond to the homogenization, saturation and setting stages. During homogenization, the flow resistance decreased sharply and then remained constant during saturation. As setting began, flow resistance increased quickly. Similar changes are observed with H value measurements, although not synchronized in time.

3.3 Matrix

The Bohlin rheometer was used to measure slurry rheology for times up to 360 min. The shear rates were much different in magnitude, being 400 times larger when considering the matrix slurry only.

The relation between shear stress and shear rate is shown in Fig. 7. The shear stress increased with increasing shear rates. The shear stress and apparent viscosity value were higher during the forward cycle than the reverse cycle, leading to the formation of successive hysteresis loops.

The loops of matrix slurry shifted downward from 0 h to 3 h and then increased to 6 hr. The shear stress (τ_{max}) at the highest shear rate of 400 s⁻¹, at different testing times, is given in Table 3. The τ_{max} decreased slightly and then increased. The same trend was observed for the torque (T_{max}) at the highest impeller speed of 1.10 s⁻¹ at different testing times, as given in Table 2. The forward cycle revealed pseudoplastic behavior of the slurry, while the reverse cycle displayed almost Bingham behavior.

The apparent viscosity as a function of shear rate for the matrix slurry at different times is shown in Fig. 8. The apparent viscosity in the forward cycle (shear rate increasing) was higher than in the reverse cycle (shear rate decreasing). In the forward cycle, the apparent viscosity at different aging times decreased sharply from 0 to 5.0 s⁻¹ and remained similar until 100 s⁻¹ then decreased until 400 s⁻¹. The apparent viscosity at 0 h is the highest and decreases at 1 h, 2 h and 3 h at shear rates below 5.0 s⁻¹. At shear rates higher than 5.0 s⁻¹, the apparent viscosity at different aging times remained almost constant. In the reverse cycle, the apparent viscosity remained similar from the shear rate of 400 s⁻¹ to 1⁻¹ and then increased at very low shear rate. At higher shear rates, all values of apparent viscosity merge at of 0.7 Pa•s.

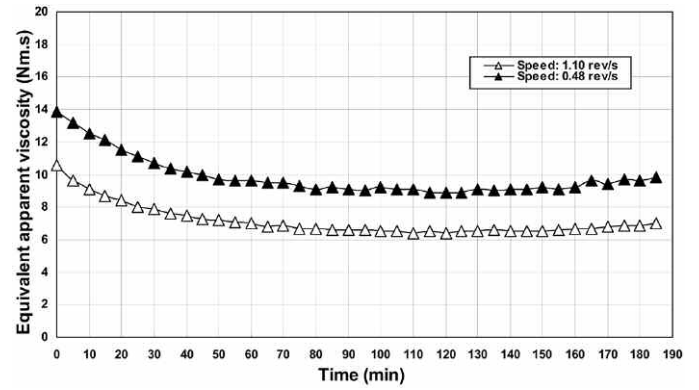


Fig. 5. Equivalent apparent viscosity vs. time at high and low impeller speed.

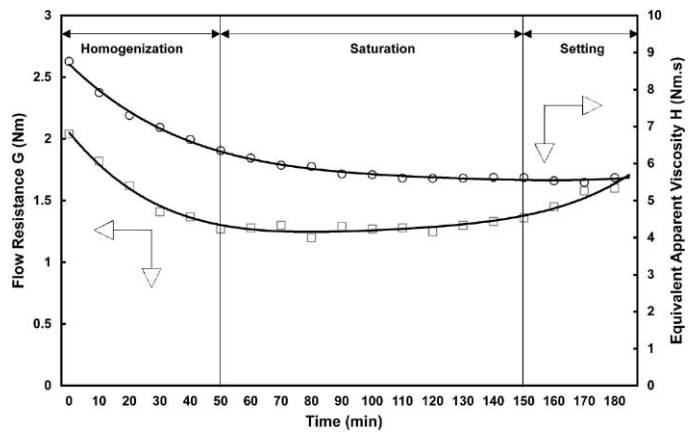


Fig. 6. Flow resistance and apparent viscosity at different times.

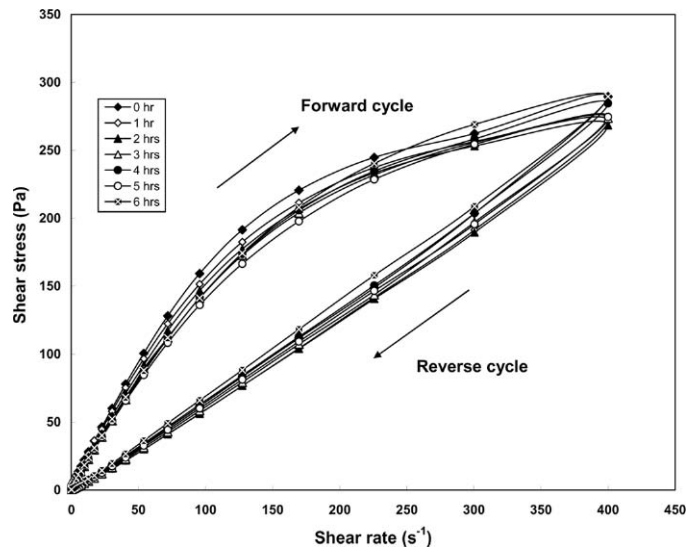


Fig. 7. Shear stress vs. shear rate for the matrix slurry at different times.

Table 4. Plastic viscosity and yield stress at different time

Time (hr)	0	1	2	3	4	5	6
Plastic viscosity (Pa•s)	1.83	1.78	1.69	1.62	1.59	1.57	1.63
Plastic yield stress (Pa)	3.51	3.00	2.12	1.51	1.67	1.88	1.93

If the viscosity decreases as the shear rate is increases, the material is said to be shear thinning or pseudoplastic. The opposite effect is known as shear thickening. Thickening is often associated with an increase in sample volume, which is termed dilatancy. The relationship between apparent viscosity and time at constant shear rate is shown in **Fig. 9**. At the constant shear rate, the apparent viscosity decreases with time and then stabilizes and this effect is clearer at high shear rates. The apparent viscosity is higher at low shear rate than at high shear rate. This confirms the thixotropic behavior for the mix.⁷

Thixotropy is closely related to shear-thinning and is usually expected in yield-shear thinning suspensions where disruption of the gelation from the shearing action reduces the measured viscosity.⁷ The higher the shear rate, the more effectively the gel is broken down, and the lower the measured viscosity. Although gel structures break down under shear, the structures will reform with time. Suspension properties, relating to particle physics and interparticle chemistry, determine the rate at which the gel will form. Gelation rate rebuilds the gel structure and balances with shear rate that breaks down the gel structure. The minimum viscosity achieved by a system at constant shear rate will occur at the balance point between these two phenomena. Degree of thixotropy has been quantified by using the following formula:²⁸

$$\Delta T = \sum (\tau^{\text{up}} - \tau^{\text{down}}) \quad (5)$$

where at the same shear rate, ΔT is thixotropy degree (Pa), τ^{up} is shear stress - forward cycle (Pa) and τ^{down} is shear stress - reverse cycle (Pa).

The loop area of a rheogram is calculated, using the following formula:

$$S = 0.5 \cdot \sum (\gamma_{i+1} - \gamma_i) \cdot \sum (\tau^{\text{up}}_{i+1} - \tau^{\text{up}}_i + \tau^{\text{down}}_{i+1} - \tau^{\text{down}}_i) \quad (6)$$

where S is loop area (Pa/s), γ_i is shear rate at the i^{th} point (s^{-1}), γ_{i+1} is shear rate at $i+1^{\text{th}}$ point (s^{-1}), τ^{up}_{i+1} is shear stress at $i+1^{\text{th}}$ point in forward cycle (Pa), τ^{up}_i is shear stress at i^{th} point in forward cycle (Pa), τ^{down}_{i+1} is shear stress at $i+1^{\text{th}}$ point in reverse cycle (Pa), τ^{down}_i is shear stress at i^{th} point in reverse cycle (Pa).

The degree of thixotropy decreased from the 0 to 4 h and then remained stable, as shown in **Fig. 10**. There was no significant decrease in the first hour. The loop area values followed the same trend.

For a typical plastic flow curve, shown in **Fig. 11**, the plastic yield stress, τ_p , corresponds to the intercept of the extrapolated straight line to ordinate (τ - γ plot) and the slope corresponds to the plastic viscosity η_p . For good flowability, both τ_y and η_p should be low. For a castable, however, water should not be used to achieve the lower values. For a high packing fraction suspension at a certain consistency, various deflocculants will have an impact on these two parameters. When all other things are equal, lower τ_y and η_p will yield better flowability.

In **Fig.11**, plastic yield stress and viscosity are calculated from shear rate 0.556 to 54.024 s^{-1} and the correlation is quite good. The calculated values of plastic yield stress decreased with time and stabilized after 4 h. Plastic viscosity decreased with time until 4 h and then increased slightly, as given in **Table 4**. This is of course related to the hydration reactions of CAC.

3.4 Conductivity

The conductivity results are shown in **Fig. 12**. From 0 (point A) to 10 min (point B), the conductivity drastically increased due to the fast dissolution of the dispersant SHMP present in the system. After this, from 10 to 150 min (point C), the conductivity increased very slowly because of the dissolution of CAC. From 150 min to 345 min (point D), the conductivity increased sharply and reached a peak. At 345 min, nucleation started, followed by massive precipitation at 415 min (point E). After the massive precipitation occurred, the conductivity decreased. Subsequently, after a slight increase, the conductivity remained constant. This represented an equilibrium between anhydrous and hydrated phases in solution. In this experiment, the delayed dissolution of cement from Point B to C was due to the presence of fine fillers, which cover the cement grains. Moreover, the deposition of cal-

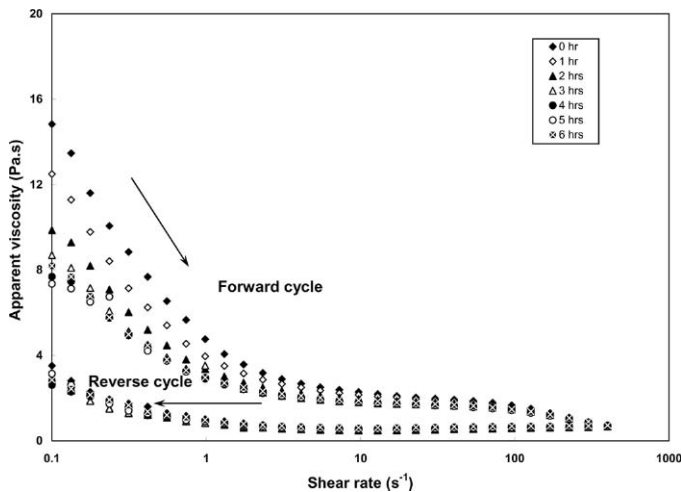


Fig. 8. Apparent viscosity vs. shear rate for the matrix slurry at different time.

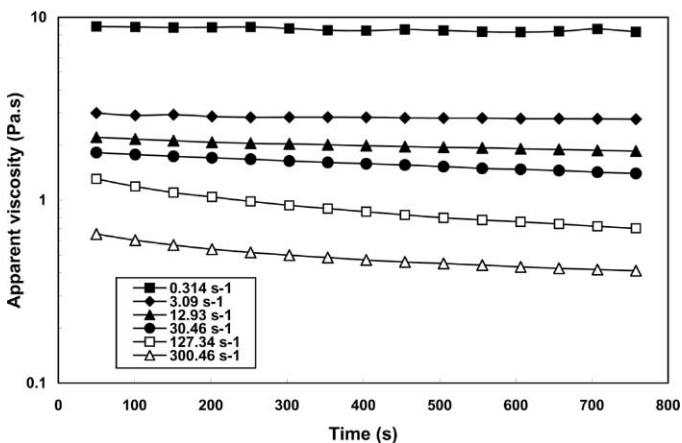


Fig. 9. Apparent viscosity of the matrix slurry at different constant shear rates.

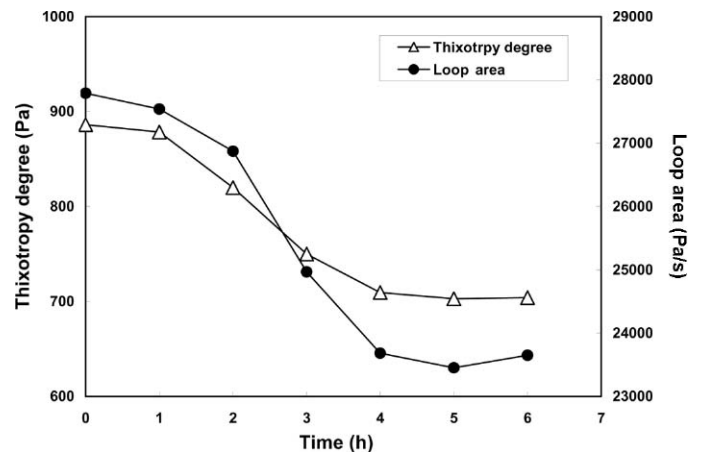


Fig. 10. Thixotropy degree and loop area for the matrix slurry at different time.

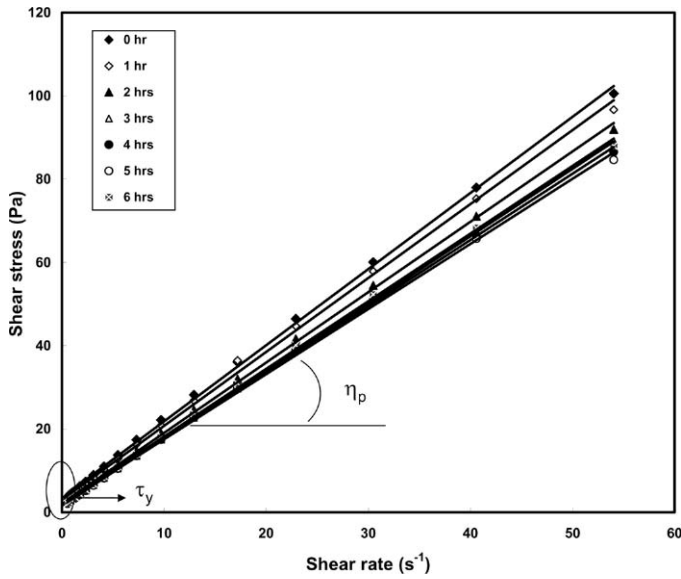


Fig. 11. Yield stress and plastic viscosity of the matrix slurry at different times.

Table 4. Plastic viscosity and yield stress at different time

Time (hr)	0	1	2	3	4	5	6
Plastic viscosity (Pa*s)	1.83	1.78	1.69	1.62	1.59	1.57	1.63
Plastic yield stress (Pa)	3.51	3.00	2.12	1.51	1.67	1.88	1.93

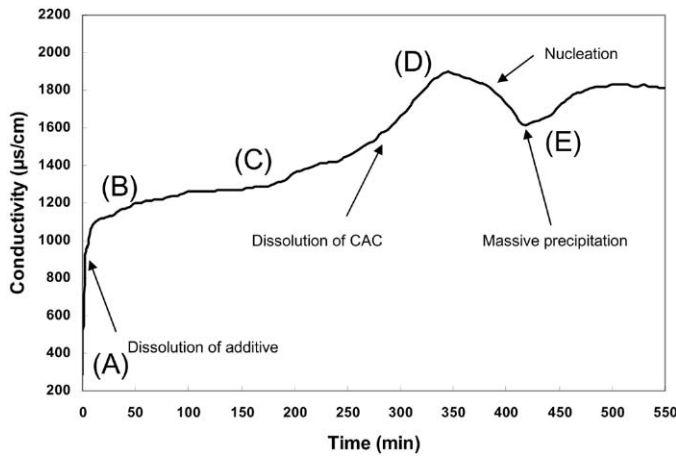


Fig. 12. Conductivity curve of the matrix with a water / solid ratio of 2.5 at 20 °C.

cium phosphate also hindered dissolution of CAC grains. Microsilica can also play a key role by interacting with the surface of the cement grain forming a diffusion layer that could delay the dissolution of CAC grains.^{16,29}

3.5 Exothermic Profile

During curing, the castable mix temperature and room temperature were measured and the data are shown in Fig. 13. The room temperature slightly fluctuated around 20°C (point A). Two heat evolution peaks were observed for the castable mix. After the castable was wet-mixed for 4 min, the temperature reached 23°C (point B) in a short time. The castable temperature remained stable for 6 h (point C) and then increased sharply to reach a first peak at 25.0°C after 7 h (point D). The castable mix temperature then increased to a maximum of 29.3°C (the second peak) after 11 h (point E). Further on, the castable tem-

perature slowly decreased until the end (point F). The time measured from the start of mixing (zero) until the exothermic reaction showed a temperature increase of + 5.0°C was recorded (EXO+5). For CA-14 cement, this point corresponds to the Vicat final setting time. The time when the castable mix had reached its maximum temperature was also recorded (EXO max). This point corresponds to the time when there is sufficient green strength for demolding.³⁰ In Fig. 13, the EXO+5 is presented by point D at the time of 7 h and the EXO max is presented by point E with the period of 11 h. From point A to B, the temperature increased because of the dissolution of additives. From B to C, the temperature remained the same, during the slow dissolution of CAC. From C to D, the temperature increased to the first peak (point D) indicating that the final setting had started with hydrate product crystallization as shown in Fig. 12. From point D to E, the temperature increased to a maximum indicating that sufficient demolding strength had developed. From point E to F, the castable temperature decreased as the hydrated products of CAC reached equilibrium and crystallized slowly.

3.6 Discussion

There are a few practical difficulties in carrying out the rheological tests of matrix slurry and castable under similar conditions. The most important is protection of water from evaporation while testing. The rheological test on castable was carried out in open atmosphere without protection from water evaporation, while the fine matrix rheology was conducted under a protecting atmosphere.

Variation of water to cement ratio is possible, when introducing coarse grains into the fine matrix as grain porosity absorbs water from the fine matrix. The rheology of matrix and castable are to be compared keeping these variations in mind. Flow resistance, (G) of a castable are compared with the plastic yield stress (τ_p) of the matrix slurry as shown in Fig. 14.

Similarly, torque viscosity (H) is compared with plastic viscosity (η_p) in Fig. 15. The curves show similar trends but at different times because of the differing test conditions. Comparison of T_{max} (Table 2) and τ_{max} (Table 3) with aging time is similar and hence is not shown.

The delay in bulk dissolution of CAC, observed initially in conductivity data (Fig. 12), corresponds to extension of working time. This corresponds to the period in the castable rheology study where flow resistance remains stable as shown in Fig. 6.

Variation of plastic viscosity and yield stress with time (Table 4) as well as reduction in the degree of thixotropy for the matrix slurry (Fig. 10) were slow in the first hour, and then decreased noticeably between hours 1 and 5. This is to be correlated with the initial temperature inertia noticed in the exothermic profile curve, Fig. 13, up to point C, followed by the fluctuations from points

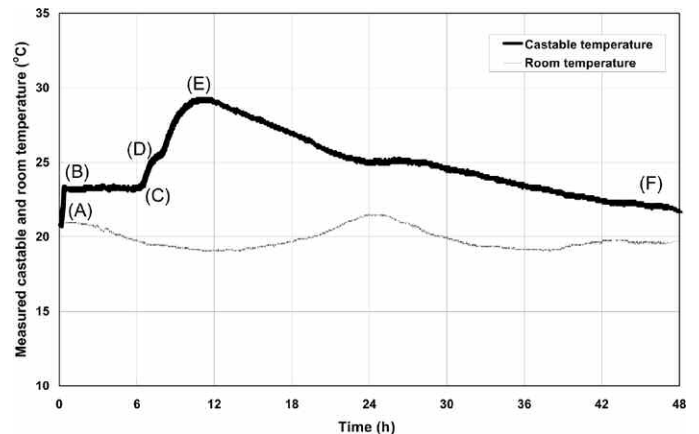


Fig. 13. Exothermic profile of the castable at 20°C.

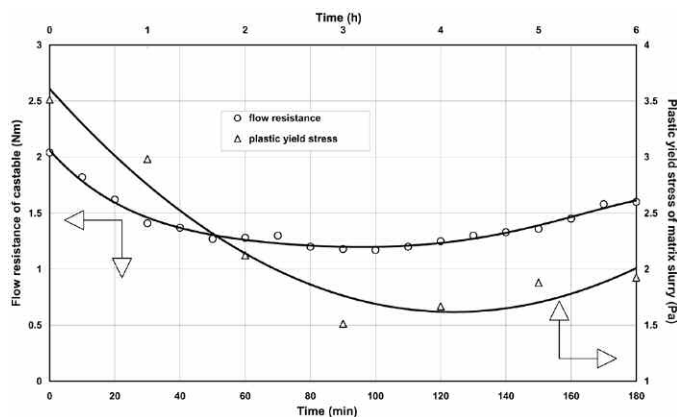


Fig. 14. Flow resistance of the castable and plastic yield stress of the matrix slurry at different times.

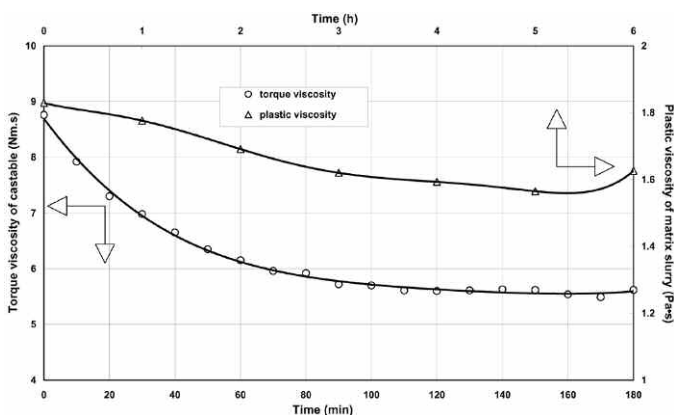


Fig. 15. Torque viscosity of the castable and plastic viscosity of the matrix slurry at different aging times.

C to E. The main difference is only in the time scale, the exothermic effect in the castable being much more sluggish.

3.7 Conclusions

The rheological behavior of bauxite based low-cement castable and its fine matrix has been studied using different rheometers. The conclusions based on this investigation are:

- The castable mix has shown pseudoplastic and Bingham behaviors. The thixotropy has been observed when analyzed with testing time at constant impeller speed. Similar behavior has been observed with τ_p and η_p of the matrix slurry.
- During aging, the rheological characteristics change from a homogeneous to saturation and then to setting controlled.
- Comparison of rheological results of the castable and matrix slurry between G-H and τ_p - η_p values shows similarity in trends but at different aging times. The castable and matrix rheology are correlated with conductivity and exothermic profile studies.

ACKNOWLEDGEMENTS

The authors extend their sincere thanks to Prof. P. J. Carreau, Director of Applied Polymer Research Centre at École Polytechnique, for use of the Bohlin CVO 120 HR rheometer and to F. Cotton for his technical assistance.

References

- W. W. Wright, "The Effect of High Temperature Phases on Low and Ultra Low Cement Castables Hot Properties," Ph. D. Thesis, Monash University, 6-16 (2000).
- K. Fujii, W. Kondo and H. Ueno, "Kinetics of Hydration of Monocalcium Aluminate," *J. Am. Ceram. Soc.*, **69** [4] 361-364 (1986).
- C. D. Parr, C. Revais and H. Fryda, "The Nature of Chemical Reactions That Occur During castable Installation and Analytical Techniques Used to Follow These Reactions," *Fundamentals of Refractory Technology*, Ceramic Transactions Vol. 125, Ed. J. P. Bennett and J. D. Smith, The American Ceramic Society, 2001, 53-71.
- A. Nishikawa, Editor, *Technology of Monolithic Refractories*, Pub. Plibrico Japan Company limited, Japan, 1984, 598.
- Y. Sasagawa, M. Sato and K. Nozawa, "Role of Alumina Cement in Castable Refractories," *Proc. of UNITECR '95*, Kyoto, Japan, Vol. 2, 1995, 301-308.
- C. Parr, R. Roseky, C. Wöhrmeyer, "Calcium Aluminate Cements for Unshaped refractories", *CN Refractories Special Issues Vol. 5*, 2001, 6-12.
- J. E. Funk and D. R. Dinger, "Predictive Process Control of Crowded Particulate Suspensions, Applied to Ceramic Manufacturing," Kluwer Academic Publishers, 1994, 327-371.
- K. Watanabe, M. Ishikawa and M. Wakamatsu, "Rheology of Castable Refractories," *Taikabutsu Overseas*, **9** [1] 41-53 (1989).
- N. Zhou, "Elaboration of Al₂O₃-based Graphite Containing Castables," Ph.D. Thesis, University of Montreal, Canada, 105-119 (2000).
- Hemphill, W. Campos and A. Pilehvari, "Yield-Power Law Model More Accurately Predicts Mud Rheology," *Oil & Gas Journal*, **91** [34] 45-50 (1993).
- C. F. Ferraris, "Measurement of the Rheological Properties of High Performance Concrete: State of the Art Report," *Journal of Research of the National Institute of Standard and Technology*, **104** [5] 461-478 (1999).
- C. F. Ferraris, F. de Larrard and N. Martys, "Fresh Concrete Rheology: Recent Developments, Materials Science of Concrete VI," S. Mindess and J. Skalny, eds., The American Ceramic Society, 215-241, (2001).
- V. A. Hackley and C. F. Ferraris, National Institute of Standard and Technology Special Publication 946, *Guide to Rheological Nomenclature: Measurements in Ceramic Particulate Systems*, 31 pages, 2001.
- C. Parr, C. Wöhrmeyer, B. Valdelièvre and A. Namba, "Effect of Formulation Parameters upon the strength Development of Calcium Aluminate Cement Containing Castables," *Journal of the Technical Association of Refractories, Jpn.*, **23** [4] 231-238 (2003).
- R. Funakoshi, T. Mastue, N. Takahashi and M. Ishikawa, "A Study of the Setting Mechanisms of Low-cement Castables by Exothermic Profile," *J. Tech. Assoc. Refractories, Jpn.*, **23** [4] 286-289 (2003).
- C. Alt, C. Parr and C. Revais, "The Effect of Environmental Temperature Conditions on the Rheology of Deflocculated Refractory Castable," *RA&N*, **7** [1] 9-15 (2002).
- Z. Q. Chen, B. Myhre and B. Sandberg, "Flow and Flow Decay of Refractory Castables," *China's Refractories*, Vol. 12(4), 2003, 16-19.
- C. Parr, B. Valdelièvre and C. Wöhrmeyer, "Application of Calcium Aluminate Cement to Dense Low Water Demand Refractory Castables," *RA&N*, **7** [3] 17-23 (2002).
- P. C. Evangelista, C. Parr and C. Revais, "Control of Formulation and Optimization of Self-flow Castables Based on Pure Calcium Aluminates," *RA&N*, **7** [2] 14-18 (2002).
- V. Jones, "Flow Control of Low-cement Self-flow Castables", *Proc. of the Unified International Technical Conference on Refractories*, Nov. 4-7, 1997, New Orleans, USA, Vol. 2, 635-644.
- ASTM C1446-99, "Standard Test Method for Measuring Consistency and Working Time of Self-flowing Castable Refractories," *ASTM International*, Vol. 15.01.
- R. G. Pileggi, V. C. Pandolfelli, A. E. Paiva, J. Gallo, "Novel Rheometer for Refractory Castables," *Am. Ceram. Soc. Bull.*, **79** [1] 54-58 (2000).
- R. G. Pileggi, A. R. Studart, V. C. Pandolfelli, J. Gallo, "How Mixing Affects the Rheology of Refractory Castables," *Am. Ceram. Soc. Bull.*, Part 1, **80** [6] 27-31 (2001), Part 2, **80** [7] 38-42 (2001).
- X. X. Zhou, K. Sankaranarayanan and M. Rigaud, "Design of Bauxite-based Low-cement Pumpable Castable: A Rheological Approach", *Ceramics International*, **30** [1] 47-55 (2004).
- X. Zhou, K. Sankaranarayanan, M. Rigaud, N. Zhou, S. Zhang, "Effect of Microsilica on Rheological behavior of Bauxite-Based Low-Cement Pumpable Castable," *Interceram*, **53** [3] 166-173 (2004).
- X. Zhou, "Rheology of Bauxite-based Low-cement Shotcreting Castables," Ph.D. Thesis, University of Montreal, Canada, 253 Pages (2004).
- D. Beaupré, "Rheology of High Performance Shotcrete," Ph. D. Thesis, the University of British Columbia, Canada, (1994).
- A. Q. Ma, M. S. Liu, M. X. Jiang, et al., "Factors Influencing the Thixotropy of High Alumina Castable Slurry," *China's Refractories*, **37** [2] 89-91 (2002).
- C. D. Parr, C. Revais and H. Fryda, "The Nature of Chemical Reactions That Occur During castable Installation and Analytical Techniques Used to Follow These Reactions, Fundamentals of Refractory Technology," *Ceramic Transactions*, Ed. J. P. Bennett and J. D. Smith, The American Ceramic Society, Vol. 125, 2001, 53-71.
- Alcoa Industrial Chemicals (ALMATIS), *Product Data: Calcium Aluminate Cements (GP/005/R00/1001/MSDS 993)*, 1999.